University of Pennsylvania
ScholarlyCommons

Departmental Papers (CBE)

Department of Chemical & Biomolecular Engineering

February 2008

# Analysis of the Performance of the Electrodes in a Natural Gas Assisted Steam Electrolysis Cell

Wensheng Wang
*University of Pennsylvania*

Raymond J. Gorte
*University of Pennsylvania*, gorte@seas.upenn.edu

John M. Vohs
*University of Pennsylvania*, vohs@seas.upenn.edu

Follow this and additional works at: http://repository.upenn.edu/cbe_papers

Recommended Citation
Wang, W., Gorte, R. J., & Vohs, J. M. (2008). Analysis of the Performance of the Electrodes in a Natural Gas Assisted Steam Electrolysis Cell. Retrieved from http://repository.upenn.edu/cbe_papers/106

Postprint version. Published in *Chemical Engineering Science*, Volume 63, Issue 3, February 2008, pages 765-769.
Publisher URL: http://dx.doi.org/10.1016/j.ces.2007.10.026

This paper is posted at ScholarlyCommons. http://repository.upenn.edu/cbe_papers/106
For more information, please contact repository@pobox.upenn.edu.

# Analysis of the Performance of the Electrodes in a Natural Gas Assisted Steam Electrolysis Cell

**Abstract**

The performance of solid oxide electrolysis (SOE) cells while operating in the natural gas assisted steam electrolysis (NGASE) mode was evaluated. The SOE cells used yttria-stabilized-zirconia (YSZ) as the oxygen ion conducting electrolyte, Co–$CeO_2$–YSZ as the $H_2$–$H_2O$ electrode, and Pd-doped **$CeO_2$ YSZ** source as the $CH_4$-oxidation electrode. The cell electrochemical performance was evaluated as a function of the $H_2O/H_2$ ratio and the extent of conversion of $CH_4$. The results of this study provide insight into the factors that control electrode performance and further demonstrate the viability of an NGASE cell for the production of $H_2$.

**Keywords**

catalysis, electrolysis, energy, fuel, hydrogen production, steam

**Comments**

Postprint version. Published in *Chemical Engineering Science*, Volume 63, Issue 3, February 2008, pages 765-769.

Publisher URL: http://dx.doi.org/10.1016/j.ces.2007.10.026

This journal article is available at ScholarlyCommons: http://repository.upenn.edu/cbe_papers/106

# Analysis of the Performance of the Electrodes in a Natural Gas Assisted Steam Electrolysis Cell

Wensheng Wang, Raymond J. Gorte, and John M. Vohs *

Department of Chemical and Biomolecular Engineering

University of Pennsylvania

Philadelphia, PA 19104

## Abstract

The performance of solid oxide electrolysis (SOE) cells while operating in the natural gas assisted steam electrolysis (NGASE) mode was evaluated. The SOE cells used yttria-stabilized-zirconia (YSZ) as the oxygen ion conducting electrolyte, Co-$CeO_2$-YSZ as the $H_2$-$H_2O$ electrode Pd-doped, $CeO_2$-YSZ $CH_4$-oxidation electrode. The cell electrochemical performance was evaluated as a function of the $H_2O/H_2$ ratio and the extent of conversion of $CH_4$. The results of this study provide insight into the factors that control electrode performance and further demonstrate the viability of an NGASE cell for the production of $H_2$.

**Keywords**: catalysis, electrolysis, energy, fuel, hydrogen production, steam

* Correspondence author, Email: vohs@seas.upenn.edu

## Introduction

Solid oxide electrolyzers (SOE) have the potential to be efficient devices for the production of high purity hydrogen from water. The ability to produce hydrogen free from impurities other than water is particularly attractive for polymer exchange membrane (PEM) fuel cells where the electrodes are highly susceptible to poisoning by impurities such as CO and sulfur. In a SOE water or a mixture of water and hydrogen is fed to the cathode where the water is dissociated to produce $H_2$ and oxygen anions that are transported through an oxygen ion conducting ceramic electrolyte (typically yttria-stabilized zirconia, YSZ) to the anode. In conventional designs molecular oxygen is evolved into an air stream on the anode and, thus, the oxygen partial pressure on the anode is significantly higher than that on the cathode producing a large chemical potential barrier for the transport of oxygen through the electrolyte. In order to overcome this barrier an external power supply must be used to "pump" the oxygen anions through the electrolyte. The chemical potential difference between the cathode and the anode and the external electrical power requirement can be reduced significantly by exposing the anode to a reducing gas such as methane that can react with the evolved oxygen. This approach is called natural gas assisted steam electrolysis (NGASE) [Martinez-Frias et al., 2003]. A schematic diagram of an NGASE cell is displayed in Figure 1. Note that the overall reaction being performed in an NGASE cell is equivalent to the steam reforming of methane followed by water gas shift. This is accomplished, however, in a single membrane reactor that separates the $CH_4/CO_2$ stream from the $H_2/H_2O$ stream, thereby eliminating the need for difficult gas phase separations in order to produce pure $H_2$.

Another advantage of NGASE is that, at least for some operating conditions, the Nernst potential is positive and the electrolysis reaction will proceed without application of an external potential. Efficient operation in this mode requires, however, electrodes that have high activity for methane oxidation and are stable when exposed to hydrocarbons under reducing conditions. This latter constraint rules out Ni/YSZ cermet electrodes that are commonly used in solid oxide fuel cells (SOFC) since they catalyze the formation of carbon deposits from methane which rapidly degrades performance. Our group has developed alternative electrode designs that circumvent this problem by either replacing Ni with Cu which is not prone to coking [Gorte et al., 2000; Kim et al,. 2001; Lu et al., 2003] or using all ceramic electrode formulations [Gross et al., 2007; Gross et al., 2007]. For example, we have shown that electrodes based on thin porous YSZ layers that are impregnated with high loadings of $CeO_2$ (40 wt %) and dopant levels of a catalytically active metal such as Pd exhibit excellent performance on both $H_2$ and $CH_4$ in SOFCs [Gross et al., 2007; Gross et al., 2007]. One of the objectives of the work presented here was to evaluate the performance of electrodes of this design in an NGASE cell. Since there have been very few studies of electrolysis cells operating in the NGASE mode a second objective was to evaluate how the performance of the anode and cathode in an NGASE cell vary as a function of the fuel utilization (i.e. anode and cathode gas composition). This insight is needed to further evaluate the potential of the NGASE approach and to predict the overall performance and efficiency of this type of hydrogen production device.

## Experimental

Two identical solid oxide electrolysis cells were used in this investigation and were constructed using a three-layer YSZ (8 mole % yttria) disc which consisted of a dense YSZ electrolyte layer sandwiched between two porous electrode layers. The multi-layer disc was fabricated by laminating three YSZ tapes. The center electrolyte tape contained only YSZ and organic binders, while sacrificial pore formers (graphite and/or polyethylene) were included in the tapes used for the anode and cathode. The tapes were laminated under a pressure of ~6 MPa at 340 K and then sintered to 1773 K. During firing the pore formers combusted resulting in a dense, 50 μm thick YSZ electrolyte disc, 1.25 cm in diameter, sandwiched between 15 μm and 300 μm thick porous YSZ layers.

The active components of both electrodes were added using wet impregnation as has been described in detail previously [Huang et al., 2004, 2004, 2005; Lee et al., 2004, 2005; McIntosh et al., 2003; Costa-Nunes et al., 2005]. The 300-μm thick porous electrodes were loaded with 15 wt % $CeO_2$ and 30 wt % Co by impregnation of aqueous solutions of $Co(NO_3)_2$ and $Ce(NO_3)_3$. The 15-μm thick porous electrodes were loaded with 40 wt% $CeO_2$ and 1 wt % Pd by impregnation of aqueous solutions of $Ce(NO_3)_3$ and $(NH_3)_4Pd(NO_3)_2$. The 15-μm electrode had an active area of 0.35 $cm^2$. The electrical conductivity in the thinner electrode was supplied by the ceria and the Pd dopant was used to enhance the catalytic activity for the oxidation of $CH_4$. We have previously shown that SOFC anodes of this design exhibit high performance for the direct oxidation of hydrocarbon-based fuels [Gross et al., 2007].

Electrical contacts were made using Ag wire and Ag paste on both electrodes. The cells were sealed onto 1.0 cm diameter alumina tubes using a ceramic adhesive (Aremco,

Ultra-Temp 516) with the anode on the inside of the tube. This tube was then placed into a second larger tube that was sealed at one end. This two-tube set-up allowed the composition and flow rates of the gasses exposed to both electrodes to be controlled. During electrolysis cell testing the Co-ceria-YSZ electrode was exposed to streams containing mixtures of $H_2O$ and $H_2$. In some experiments $N_2$ was included as a diluent. While the flow rate of the carrier gas was maintained at 130 ml/min, the flow rate of the gas sent to the Co-ceria-YSZ electrode varied from 130 to 360 ml/min depending on steam content. The feed gas to the Pd-ceria-YSZ electrode consisted of mixtures of $CH_4$, $H_2O$, and $CO_2$. Since it was not possible to operate the button cells used in this study at high conversions, $CO_2$ was added to the anode feed gas in order to simulate the gas composition at high conversions. For example, a mixture of $CH_4$ **:**$H_2O$**:**$CO_2$.=10**:**40**:**80 was used to simulate 80% conversion. Because the flow of oxygen ions was negligible compared to the gas flow rates, conversion in each compartment was truly differential, so that analysis of exit-gas compositions was not useful.

In addition to being an excellent hydrocarbon oxidation catalyst, Pd/$CeO_2$ has high activity for steam reforming of methane [Wang and Gorte, 2001]. Thus, some reforming of the methane will occur on the anode. Since the residence time for the gas in the button cell is short, the extent of reforming in the anode is likely to be relatively low. This would not be the case, however, in larger cells running at high conversions where the amount of steam reforming will be much higher. Therefore, in order to more accurately simulate the gas compositions that would be present under realistic operating conditions, the anode gas was passed through a small pre-reactor containing a Pd/$CeO_2$ catalyst prior to being sent to the electrolysis cell in order to allow the gas-phase

composition to come to equilibrium. The pre-reactor was maintained at the same temperature as the electrolysis cell. To calculate values of the OCV for each operating condition we assumed that the following reforming reactions came to equilibrium within the pre-reactor (only reaction 1 was used when the Pd-ceria-YSZ electrode was exposed to only $CH_4$ and $H_2O$):

$$H_2O + CH_4 \Leftrightarrow CO + 3H_2 \qquad (1)$$

$$H_2O + CO \Leftrightarrow CO_2 + H_2 \qquad (2).$$

V-i curves were measured over a potential range from 0.4 to -0.5 V. AC impedance data were recorded in the galvanostatic mode using a Gamry Instruments impedance spectrometer, with a frequency range from 0.01 Hz to 100 kHz and perturbation amplitude of 5 mV for various DC polarizations. Throughout this study, the $H_2O/H_2$ ratio was maintained below 13. This set the upper limits for $P_{O_2}$ at the Co-ceria-YSZ electrode to be $3\times10^{-19}$, $6\times10^{-18}$ and $9\times10^{-17}$ atm at 973, 1023 and 1073 K, respectively. These are one to two orders of magnitude lower than the equilibrium $P_{O_2}$ required for cobalt oxidation [Gaskell, 2003] insuring that cobalt remained metallic in each experiment. $N_2$ was used as a diluent for $H_2$ in order to vary the $H_2O/H_2$ ratio and $H_2O$ partial pressure over a wide range.

Because reference-electrode measurements tend to be unreliable [Adler, 2000], electrode performance was analyzed the V-i polarization curves and 2-probe impedance spectra. Electrolyte losses are certainly proportional to the current density and can be calculated from the tabulated resistivities of YSZ [Gross, et al, 2007]. It has also been previously shown that the Co-ceria-YSZ electrode exhibits an impedance that is independent of current density in $H_2$-$H_2O$ mixtures under both SOE and SOFC conditions

[Wang, et al, 2006]. Therefore, the losses within each electrode be calculated from the data provided.

While we did not perform detailed studies of electrode stability in this work, the performance of the cells remained stable for a period of at least several days at 973 K. At 1073 K, there was a gradual loss in the performance of the Pd-ceria-YSZ electrode due to a loss of conductivity associated with sintering of the ceria, as discussed elsewhere in more detail [Gross, et al, 2000].

**Results and Discussions**

The performance of the electrolysis cell was initially studied as a function of the $H_2O/H_2$ ratio and $H_2O$ partial pressure in the feed gas to the Co-ceria-YSZ electrode with the composition of the feed gas to the Pd-ceria-YSZ electrode held fixed at 97% $CH_4$ and 3% $H_2O$. As noted in the experimental section, the $CH_4$-$H_2O$ mixture was first contacted with a Pd/$CeO_2$ catalyst in order to more accurately simulate the conditions expected in a larger area cell. Figure 2 shows V-i curves obtained at 973 K for several $H_2O/H_2$ ratios. For each curve, from the OCV to 0 potential, the current flow and $H_2$ generation is driven by the chemical potential difference between the two electrodes and no external power was supplied to the cell. At negative cell potentials, an external power source was used to supply the additional potential required to maintain current flow. For $H_2O/H_2$ =13 and $P_{H_2O}$ = 0.57 atm, the measured OCV is 0.21 V and the short circuit current is 0.14 A/cm$^2$. The measured OCV for this cell is 0.36 V less than the calculated value of 0.57 V. Due to the low reactivity methane, it is likely that for high $CH_4$ concentrations equilibrium is not established in Pd-ceria-YSZ electrode and this may be the cause of the lower than expected OCV.

As shown in Figure 2, decreasing the $H_2O/H_2$ ratio to 0.9 while maintaining the $P_{H_2O}$ relatively constant at 0.53 atm resulted in an overall decrease in the cell performance. The OCV for these operating conditions was 0.13 V which is 0.33 V less than the calculated value of 0.46 V. This can again be attributed to the low reactivity of methane and equilibrium not being established on the Pd-ceria-YSZ electrode. The short circuit current for this cell condition was 0.09 A/cm$^2$. Note that the primary effect of decreasing the $H_2O/H_2$ ratio from 13 to 0.9 while holding $P_{H_2O}$ relatively constant was to decrease the OCV, which is expected based on the change in the $P_{O_2}$ with the change in the $H_2$:$H_2O$ ratio. Except at very low current densities, the slope of the V-i curve remained constant. This indicates that the kinetics of the water dissociation reaction are essentially zero order with respect to the hydrogen partial pressure, since the equal slope implies that the impedance is unchanged.

To study the dependence of $P_{H_2O}$ on the kinetics of the $H_2O$-$H_2$ reaction, the cell was also operated with a $P_{H_2O}$ of 0.1 atm and an $H_2O/H_2$ ratio of 1. The OCV for this gas composition was 0.14 V and the short circuit current was 0.055 A/cm$^2$. Note that decreasing the $P_{H_2O}$ by a factor of five from 0.53 to 0.1 atm while holding the $H_2O/H_2$ ratio nearly constant caused the cell current at each voltage to decrease by roughly 50%. While data at additional $P_{H_2O}$ values are needed to accurately determine the kinetic expression for the $H_2O$-$H_2$ reaction, this result suggests that the order of the reaction with respect to $P_{H_2O}$ is less than one. This is an important result since it indicates that it may be possible to run solid oxide water electrolysis cells at relatively high water utilizations and still obtain reasonable performance.

Figure 3 displays data on the effect of the gas composition for the $CH_4$ side on the cell performance at an operating temperature of 973 K. The goal of this series of experiments was to evaluate how the performance of the electrode varies as a function of the $CH_4$ conversion. As described in the experimental section, the gas composition for high conversions was simulated by adding $H_2O$ and $CO_2$ to the $CH_4$ feed. For example, a mixture of $CH_4$**:**$CO_2$**:**$H_2O$ = 1**:**1**:**2 was used to simulate 50% conversion. This gas stream was passed over a Pd/$CeO_2$ catalyst at the cell operating temperature in order to allow it to equilibrate and to obtain a composition that would be more representative of that present in a large area cell. The gas composition at the opposite electrode was held fixed with an $H_2O/H_2$ ratio of 13 and $P_{H_2O}$ = 0.57 atm. For comparison purposes, data is also included for gases consisting of humidified $CH_4$ (3% $H_2O$) and humidified $H_2$ (3% $H_2O$) at the Pd-ceria-YSZ electrode. These gases were also passed over the Pd/$CeO_2$ catalyst bed.

For simulated $CH_4$ conversions of 10, 50, and 80%, the measured OCVs were 0.22, 0.12, and 0.07 V respectively. These values are all within 0.1 V of those calculated using the method described above with the overall difference between the experimental and calculated values decreasing with increasing conversion. The short circuit currents for $CH_4$ conversions of 10, 50, and 80% were 0.33, 0.17, and 0.09 A/cm$^2$ respectively. It is noteworthy that the OCV is still positive even with $CH_4$ conversions as high as 80%. This indicates that the benefits of using methane as a reducing gas on the anode are maintained for relatively high $CH_4$ conversions and further demonstrates the viability of the NGASE approach.

Note that the slopes of the V-i curves for the 10, 50 and 80% $CH_4$ conversion data are nearly the same. This demonstrates that while increasing the $CH_4$ conversion lowers the OCV, it has little effect on the kinetics of the electrode reaction. This is further confirmed by the impedance data presented in Figure 4 which shows that the total area-specific resistance (ASR) of the electrodes is ~0.35 Ω $cm^2$ for the 10, 50, and 80% $CH_4$ conversions. In contrast to these results, the V-i curve for humidified $CH_4$ has a much higher slope corresponding to an ASR of 1.1 Ω $cm^2$. The origin of this difference in the electrode ASR when using humidified $CH_4$ compared to $CH_4$ streams with simulated conversion of 10% or greater becomes apparent when one examines the results obtained when exposing the Pd-ceria-YSZ electrode to humidified $H_2$ with 3% $H_2O$. Note that the V-i curves for humidified $H_2$ and 10% $CH_4$ conversion in Figure 3 are almost the same. The impedance data in Figure 4 also show that the total electrode ASR for both gasses is ~0.35 Ω $cm^2$. The most likely explanation for this similarity in the electrode performance for these two different gas compositions is that steam reforming over the Pd/$CeO_2$ catalyst results in a high concentration of $H_2$ in the 10% $CH_4$ conversion gas stream. The kinetics of the electrode reaction and the performance of the Pd-ceria-YSZ electrode are thus more representative of the operation on $H_2$ rather than that for the direct oxidation of $CH_4$. Since the electrode ASR was the same for the 50 and 80% $CH_4$ conversions, the electrode performance for these conditions also appears to be dominated by the $H_2$ oxidation reaction.

Finally, in addition to 973 K, we also investigated the performance of the NGASE cell at both 1023 and 1073 K. As expected, increasing the temperature resulted in slight increases in the OCV values and decreases in the ASR. It is useful to compare the

current obtained under short circuit conditions (0 V) as a function of temperature and $CH_4$ conversion, since this represents the transition point from where the cell runs spontaneously to where an external potential must be supplied to pump oxygen through the electrolyte. The short circuit current densities as a function of $CH_4$ conversion and temperature are listed in Table 1. These data were again obtained using a $H_2O/H_2$ ratio of 13 and $P_{H_2O}$ = 0.57 atm at the opposite electrode. For all three conversions studied the short circuit current density roughly doubled upon heating from 973 to 1073 K. Also note that for a $CH_4$ conversion of 10% a short circuit current, which corresponds to one-half the $H_2$ production rate of 0.49 A/cm$^2$, was obtained at 1073 K and decreased to 0.09 A/cm$^2$ for 80% $CH_4$ conversion. In large area NGASE cells operated at high $CH_4$ utilization, the $CH_4$ conversion will vary across the cell and therefore the hydrogen production rate would be expected to be intermediate between these two values. The performance results obtained from the button cells used in this study suggest, however, that reasonable $H_2$ production rates could be obtained in a NGASE system without the need to provide additional electrical power to pump oxygen across the electrolyte.

**Conclusions**

In this study we have investigated the effect of the electrode gas compositions on the performance of an NGASE cell with a YSZ electrolyte, a $Co/CeO_2/YSZ$ composite as the $H_2$-$H_2O$ electrode and a Pd-doped $CeO_2/YSZ$ composite as the $CH_4$ electrode. Studies of the cell performance as a function of the $H_2O/H_2$ ratio in the gas fed to the cathode indicate that the kinetics of the cathode reaction are nearly zero order in $H_2$ and less than 1$^{st}$ order in $H_2O$. Studies of the NGASE cell performance for simulated $CH_4$ conversions between 10 and 80 % showed that the kinetics of the oxidation reactions on

the Pd-doped $CeO_2$/YSZ composite anode were not a strong function of conversion. This result along with comparison to the performance when operating on humidified $H_2$ indicates that for these conditions the oxidation of $H_2$ produced by steam reforming of the $CH_4$ determines the performance of the anode. At low $CH_4$ conversions, however, direct oxidation of methane dominates and resulting in a higher ASR. Finally, the results of this study further demonstrate the viability of an NGASE cell for the production of $H_2$ and indicate that it may be possible to obtain high $H_2$ production rates without the need for applying an external potential to the cell.

**Acknowledgements**

This work was funded by the U.S. Department of Energy's Hydrogen Fuel Initiative (grant DE-FG02-05ER15721).

**References**

Costa-Nunes, O., Gorte, R.J., Vohs, J.M. , 2005. A study of direct-conversion SOFC with n-butane at higher fuel utilization. Journal of Power Sources 141, 241.

Gaskell, David R., 2003. Introduction to the Thermodynamics of Materials (4th ed.), Taylor & Francis Group

Gorte, R. J., Park, S., Vohs, J. M., Wang, C., 2000. Anodes for direct oxidation of dry hydrocarbons in a solid-oxide fuel cell. Advanced Materials (Weinheim, Ger.), 12, 1465.

Gross, M. D., Vohs, J. M., Gorte, R. J., 2007. An examination of SOFC anode functional layers based on ceria in YSZ. Journal of the Electrochemical Society 154 (7), 694-B699; 2007. A strategy for achieving high performance with SOFC ceramic anodes. Electrochemical and Solid-State Letters 10(4), 65-B69

Huang, Y., Vohs, J. M., Gorte, R. J., 2004. Fabrication of Sr-doped $LaFeO_3$ YSZ composite cathodes. Journal of the Electrochemical Society 151, A646; 2005. Characterization of LSM-YSZ composites prepared by impregnation methods. Journal of the Electrochemical Society 152, A1347; Huang, Y., Ahn, K., Vohs, J. M., Gorte, R. J., 2004. Characterization of Sr-Doped $LaCoO_3$-YSZ composites prepared by impregnation methods. Journal of the Electrochemical Society 151, A1592.

Kim, H., Park, S., Vohs, J.M., Gorte, R. J., 2001. Direct oxidation of liquid fuels in a solid oxide fuel cell. Journal of the Electrochemical Society 148, A693 .

Lee, S.-I., Vohs, J.M., Gorte, R.J., 2004. A study of SOFC anodes based on Cu-Ni and Cu-Co bimetallics in $CeO_2$-YSZ. Journal of the Electrochemical Society 151, A1319; Lee, S.-I., Ahn, K., Vohs, J.M., Gorte, R.J., 2005. Cu-Co bimetallic anodes for direct utilization of methane in SOFCs. Electrochemical and Solid-State Letters 8 (1), A48.

Lu, C., Worrell, W. L., Gorte, R. J., Vohs, J. M., 2003. SOFCs for direct oxidation of hydrocarbon fuels with samaria-doped ceria electrolyte. Journal of the Electrochemical Society 150, A354.

Martinez-Frias, J., Pham, A.-Q., Aceves, S.M., 2003. A natural gas-assisted steam electrolyzer for high-efficiency production of hydrogen. International Journal of Hydrogen Energy 28, 483.

McIntosh, S., Vohs, J.M., Gorte, R.J., 2003. Effect of precious-metal dopants on SOFC anodes for direct utilization of hydrocarbons. Electrochemical and Solid-State Letters 6, A240.

Adler, S. B., Henderson, B. T., Wilson, M. A., Taylor, D. M., Richards, R. E., 2000. Reference electrode placement and seals in electrochemical oxygen generators. Solid State Ionics, 134, 35.

Wang, X., Gorte, R. J., 2001. Steam reforming of n-butane on Pd/ceria. Catalysis Letters 73, 15.

Wang, W., Huang, Y., Jung, S.-W., Vohs, J. M., Gorte, R. J., 2006 A Comparison of LSM, LSF, and LSCo for Solid Oxide Electrolyzer Anodes. Journal of the Electrochemical Society, 153, A2066.

**Figure captions**

Figure 1. Schematic of a natural gas assisted steam electrolysis cell.

Figure 2. V-i curve as a function of composition of the cathode gas at 973 K. (○) $H_2O/H_2$=13, $P_{H_2O}$ = 0.57 atm, (◊) $H_2O/H_2$=0.9, $P_{H_2O}$ = 0.53, and (Δ) $H_2O/H_2$=1, $P_{H_2O}$ = 0.1. The anode gas consisted of $CH_4$+3%$H_2O$.

Figure 3. V-i curve as a function of anode gas composition at 973 K. Anode gas composition: (+) $H_2$+3%$H_2O$, (◊) $CH_4$, 10% conversion, (○) $CH_4$+3%$H_2O$, (Δ) $CH_4$, 50% conversion, and (X) $CH_4$, 80% conversion 80%. The cathode gas consisted had $H_2O/H_2$=13 and $P_{H_2O}$ = 0.57 atm.

Figure 4. AC impedance spectra as a function $CH_4$ conversion at 973 K. Steam electrode: $H_2O/H_2$=13, $p_{H_2O}$ = 0.57 atm.

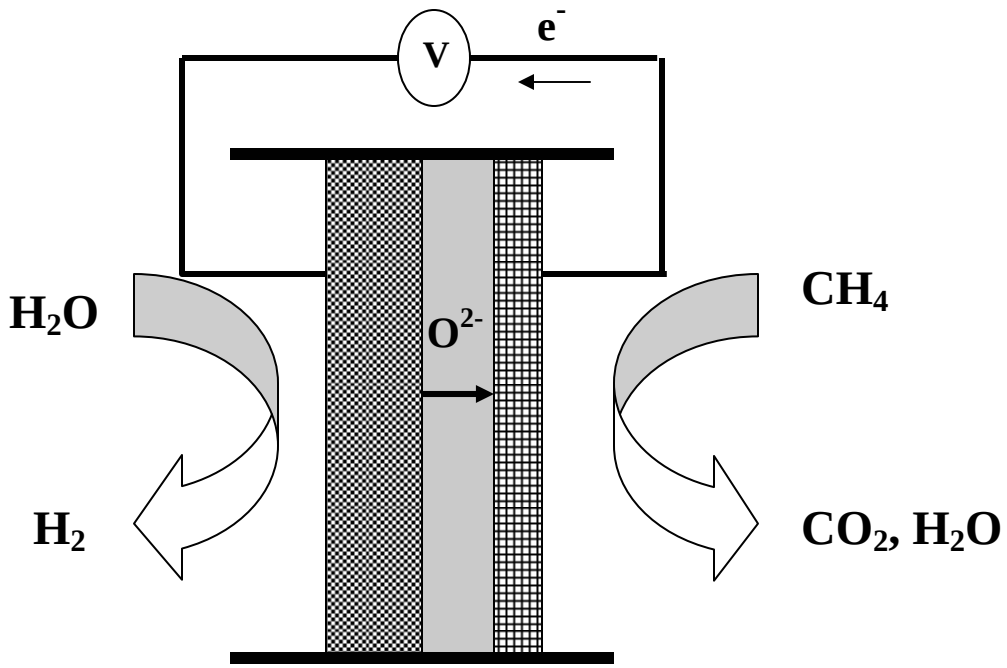


Figure 1. Schematic of a natural gas assisted steam electrolysis cell.

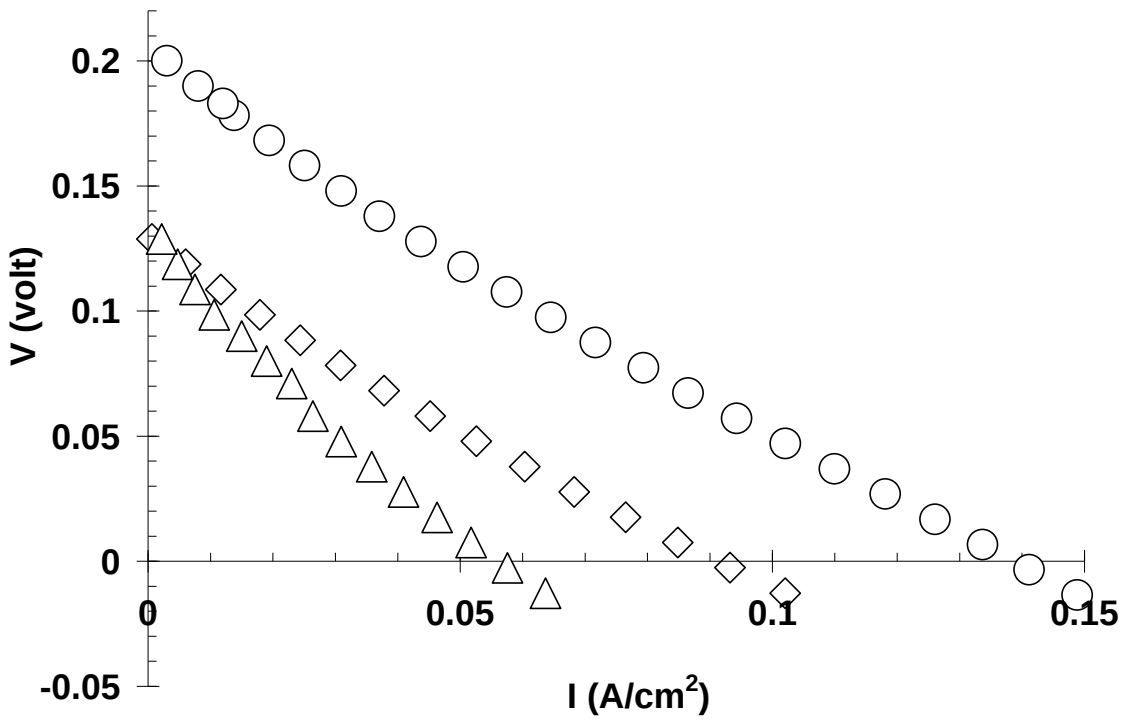


Figure 2. V-i curve as a function of composition of the cathode gas. (○) $H_2O/H_2$=13, $p_{H_2O}$ = 0.57 atm, (◊) $H_2O/H_2$=0.9, $p_{H_2O}$ = 0.53, and (Δ) $H_2O/H_2$=1, $p_{H_2O}$ = 0.1. The anode gas consisted of $CH_4$+3%$H_2O$.

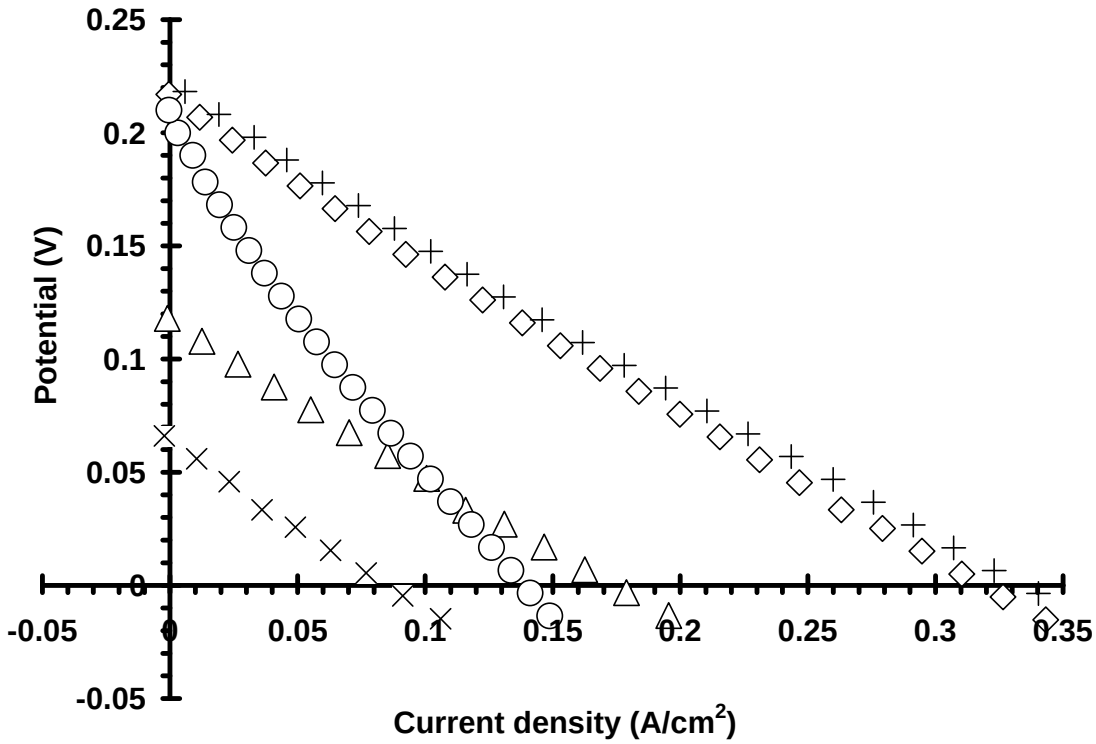


Figure 3. V-i curve as a function of anode gas composition at 973 K. Anode gas composition: (+) $H_2$+3%$H_2O$, (◊) $CH_4$, 10% conversion, (○) $CH_4$+3%$H_2O$, (Δ) $CH_4$, 50% conversion, and (X) $CH_4$, 80% conversion 80%. The cathode gas consisted had $H_2O/H_2$=13 and $p_{H_2O}$ = 0.57 atm.

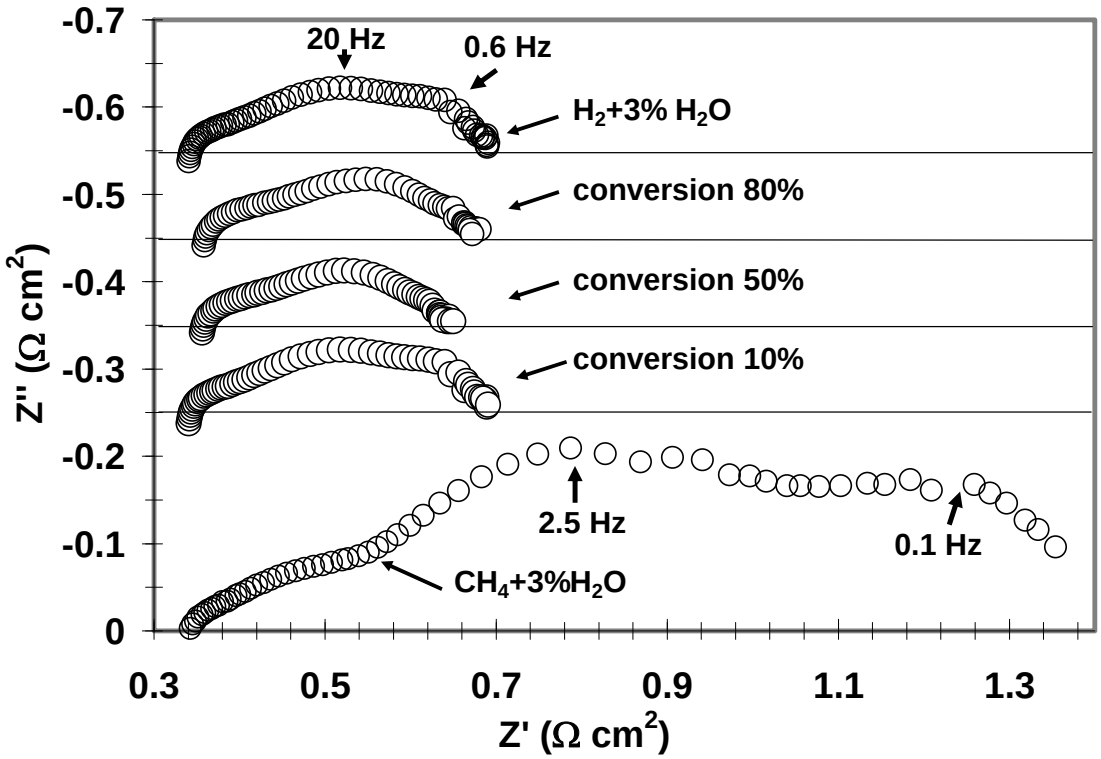


Figure 4. AC impedance spectra as a function $CH_4$ conversion at 973 K. Steam electrode: $H_2O/H_2$=13, $p_{H_2O}$ = 0.57 atm.

Table 1. The short circuit current densities as a function of $CH_4$ conversion and temperature

| | Short circuit current density ($A/cm^2$) | | |
|---|---|---|---|
| T (K) | 10% $CH_4$ conversion | 50% $CH_4$ conversion | 80% $CH_4$ conversion |
| 973 | 0.25 | 0.1 | 0.05 |
| 1023 | 0.26 | 0.14 | 0.085 |
| 1073 | 0.49 | 0.19 | 0.09 |